Quenching of excitonic quantum-well photoluminescence by intense far-infrared radiation: Free-carrier heating

J. Černe, A.G. Markelz, M.S. Sherwin, and S.J. Allen
Department of Physics and Center for Free-Electron Laser Studies, University of California, Santa Barbara, California 93106

M. Sundaram and A.C. Gossard
Materials Department, University of California, Santa Barbara, California 93106

P.C. van Son
Department of Applied Physics, Delft University of Technology, P.O. Box 5046, 2600 GA Delft, The Netherlands

D. Bimberg
Institut für Festkörperphysik, Technische Universität Berlin, Hardenbergstrasse 36, D-10623 Berlin, Germany
(Received 26 July 1994; revised manuscript received 8 November 1994)

Undoped GaAs/$Al_{0.3}Ga_{0.7}As$ and GaAs/AlAs quantum wells are simultaneously excited by weak visible light and intense far-infrared (FIR) radiation with electric fields polarized parallel to the planes of the quantum wells. The frequency of the FIR radiation ranges from 6 to 119 cm^{-1} with intensities up to 700 kW/cm^2. Peaks in the excitonic photoluminescence (PL) are broadened and quenched by the intense FIR radiation; the PL line shapes are consistent with the FIR radiation heating the carriers without significantly heating the lattice. Despite the excitonic nature of the PL, the power and frequency dependence of the carrier heating is consistent with free-carrier absorption of FIR radiation. Energy and momentum relaxation times for the free carriers are extracted from fits to a Drude model. We suggest that the FIR radiation heats free carriers that are not contributing to luminescence, and that these hot carriers in turn heat the luminescing excitons.

I. INTRODUCTION

Intense far-infrared (FIR) radiation can lead to many interesting effects in quantum wells including harmonic generation,[1,2] resonant intersubband transitions,[3] ac Stark effects,[4,5] and carrier heating.[6] These effects can be probed with excitonic photoluminescence (PL), which is sensitive to carrier dynamics.[7–9] A recent report[10] has shown that excitonic PL from undoped quantum wells can be quenched almost completely by intense FIR radiation polarized in the plane of the wells (and hence coupling only to the free, in-plane motion of the carriers). An understanding of this striking phenomenon not only provides insight into the effects of in-plane FIR electric fields on quantum-confined carriers, but serves as a prerequisite to using PL to probe the dynamics of electrons in semiconductor nanostructures in which the FIR radiation couples directly to the quantized degrees of freedom.

The confinement due to the quantum well leads electron-hole pairs to bind together to form excitons, which in turn dramatically enhance PL. Strong FIR electric fields in the plane of a quantum well can reduce PL, in principle, by exciting excitons into states where radiative recombination is diminished. A few possible mechanisms for PL quenching by FIR radiation are listed below. (1) In these samples, the exciton binding energy is expected to be between 9 and 10 meV (72–80 cm^{-1}), and, therefore, excitons could be photoionized by the FIR radiation.[10] This would decrease the electron-hole correlation, and hence decrease the PL. (2) The excitonic $1s$-$2p$ transition also is accessible to the FIR radiation. Radiative recombination for the $2p$ exciton is forbidden to the first order in perturbation theory. (3) Electrons could be separated from holes by the FIR electric field as the conduction and valence bands become tilted in the ac Franz-Keldysh effect. (4) Carrier heating could quench PL by thermally ionizing excitons,[11] or by exciting them into higher excitonic momentum states where momentum conservation restricts radiative recombination.[12]

In this paper, we investigate in detail the quenching of PL by intense FIR radiation. The sources of FIR radiation are the UCSB free-electron lasers (UCSB denotes University of California at Santa Barbara) which deliver photon energies tunable between 0.5 and 20 meV and peak powers up to 6 kW. The paper is organized as follows. Section II describes samples and experimental techniques. Section III describes experimental results. The dominant effect of the FIR radiation is to heat carriers without significantly heating the lattice. The carrier temperature (T_C) is determined by the amplitude of the PL intensity. T_C is roughly proportional to the 1/3 power of the FIR intensity. Carrier heating is more efficient at lower FIR frequencies. Section IV analyzes the carrier heating in terms of a Drude, free-carrier model. From the Drude model, energy and momentum relaxation times are extracted for various carrier tempera-

0163-1829/95/51(8)/5253(10)/$06.00

tures. The energy relaxation time is inversely proportional to the carrier temperature squared. Section V discusses the results. It is suggested that FIR radiation heats free carriers, which are not contributing to luminescence, and that these hot carriers heat the luminescing excitons. Section VI concludes with a discussion of future experiments. Two appendices are included. Appendix A highlights the relationship between carrier temperature and PL spectra, while Appendix B discusses the experimental measurement of carrier temperature using PL.

II. EXPERIMENT

A. Samples

Two undoped samples were investigated in this study. The first sample consisted of fifty 100 Å wide GaAs quantum wells between 150 Å thick $Al_{0.3}Ga_{0.7}As$ barriers. This multiple-quantum-well sample was grown by molecular beam epitaxy on a semi-insulating (100) GaAs substrate. A buffer layer consisting of 4000 Å GaAs and a smoothing superlattice were grown on top of the substrate.[10] The real-space profile of the conduction band is shown in the inset of Fig. 1(b).

The second sample contained three single GaAs quantum wells with widths of 20, 50, and 80 Å. The AlAs barriers were 180 Å wide. This structure differs from the first sample in having no Ga in the barriers and in having the growth interrupted for 100 s at the well-barrier interfaces. The sample was grown using molecular beam epitaxy on a semi-insulating GaAs substrate with a 5000 Å thick GaAs buffer layer.[9,13]

Growth interruption (GRI) at the interfaces of quantum wells greatly smooths the interfaces by allowing large islands to coalesce before the next layer is deposited. GaAs smoothes more quickly without increased trap incorporation during growth interruption, in contrast to $Ga_{1-x}Al_xAs$.[9,13] Therefore, the GaAs/AlAs sample examined here produced strong photoluminescence with several peaks corresponding to excitons recombining at interface islands (extending up to several micrometers), where the well widths differ by 1–2 monolayers (ML) [see inset of Fig. 2(b)].

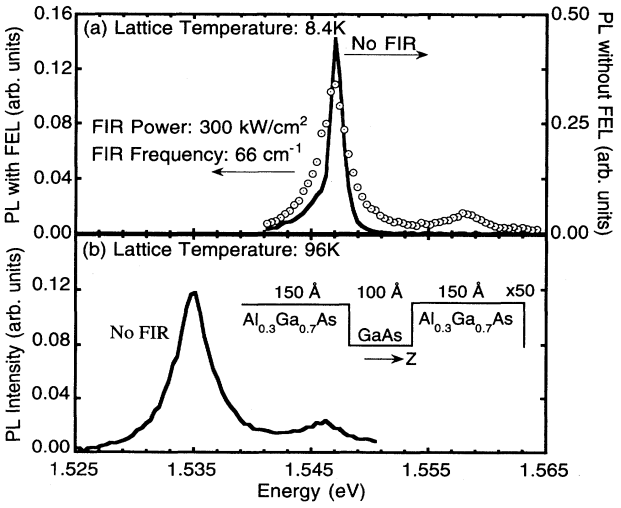

FIG. 1. Excitonic photoluminescence spectra from 100 Å wide $Al_{0.3}Ga_{0.7}As/GaAs$ multiple quantum wells (a) at 8.4 K with FIR (circles) and without FIR (solid line) irradiation, and (b) at 96 K with no FIR irradiation. Note the energy shift of the PL in (b) due to the narrower band gap at the higher lattice temperature.

B. PL Measurement

As can be seen in Fig. 3, an argon ion laser was used to excite electron-hole pairs in the undoped sample, while FIR radiation passed through the sample. The Ar^+ all-line laser excitation intensity of 10 W/cm^2 created an exciton density of approximately 3×10^9 cm^{-2} per well in the multiple-quantum-well (MQW) structure.[10] The resulting photoluminescence was captured by the same optic fiber which delivered the excitation radiation, and this luminescence was reflected off a beam splitter into a 0.34 m monochrometer and a cooled GaAs photomultiplier tube. The output of the argon ion laser was modulated acousto-optically to produce a 100 μs visible excita-

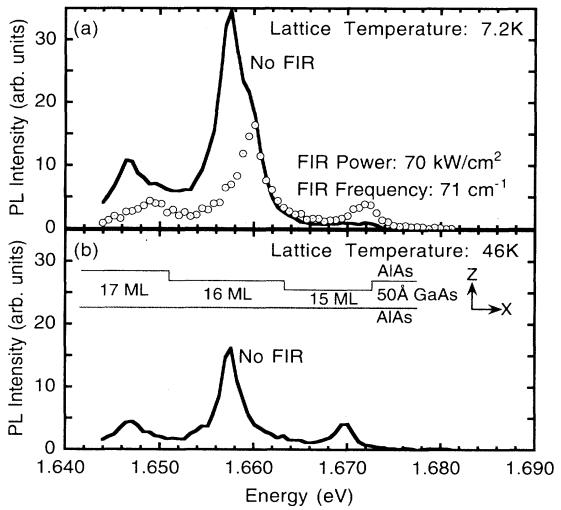

FIG. 2. Photoluminescence spectra from the 50 Å wide AlAs/GaAs growth interrupted quantum well (a) at 7.2 K with FIR (circles) and without FIR (solid line) irradiation, and (b) at 46 K with no FIR irradiation. The 1.670, 1.658, and the 1.647 meV PL peaks correspond, respectively, to radiative recombination in the 15, 16, and 17 ML wide parts of the quantum well. The PL peaks in (a) actually are doublets consisting of radiative recombination from excitons that are bound to acceptors and those that move freely in the plane of the quantum well. The high energy shoulder of the 16 ML PL peak for the solid line in (a) shows weak luminescence from free excitons. The FIR radiation in (a) thermally enhances the population of free excitons, which causes the 3 meV blueshift in the FIR-quenched PL. The PL in (b) arises from free excitons.

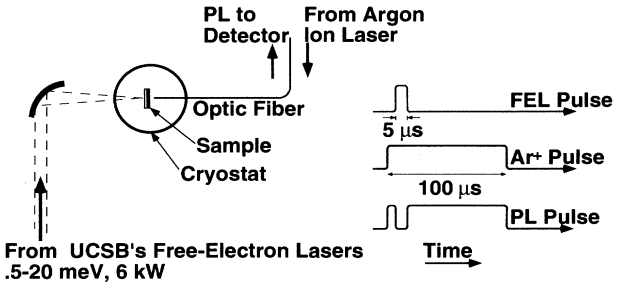

FIG. 3. A schematic of the experimental setup. Photoluminescence is detected during and after the FIR pulse has passed through the sample. The FIR radiation is polarized parallel to the plane of the quantum well. The timing of the laser pulses and PL is shown on the right side.

tion pulse that coincided with the 5 μs FIR pulse at the sample. A boxcar integrator gated the PL signal during and after the FIR pulse (see right side of Fig. 3). The unquenched, 9 K PL immediately after the FIR pulse was used to normalize all the data.

The FIR power was measured using an electrically-calibrated photothermophone energy meter (Thomas Keating Ltd.). The peak powers approached 1 kW. To obtain the intensity, the FIR spot size was measured by scanning a pyroelectric detector covered by a 200 μm aperture across the FIR focus. The spatial intensity distribution was fitted to a Gaussian. The full width at half maximum was used for the FIR spot diameter, which agreed with the diffraction limit estimates. The FIR transmission through the cryostat window and the sample substrate was included in the determination of the FIR intensity at the quantum well. No etalon effects were observed.[14] The FIR intensity was estimated to an accuracy of $\pm 20\%$.

III. RESULTS

A. Photoluminescence quenching by FIR radiation

Figures 1 and 2 illustrate the effects of lattice temperature and FIR radiation on the PL spectra from the multiple-quantum-well sample and from the GRI sample, respectively. The solid lines in Figs. 1(a) and (b) show PL spectra in the absence of FIR radiation for the multiple-quantum-well sample at 8.4 and 96 K, respectively. At 8.4 K, the PL spectrum consists of a single narrow line (FWHM < 2 meV) at 1.547 eV, which we assign to the excitonic transition from the lowest electronic state *E1* to the highest heavy-hole state HH1. At 96 K, the *E*1-HH1 transition has shifted to lower energy because the band gap narrows as lattice temperature increases, the *E1*-HH1 peak is smaller and broader, and a second peak appears at a higher energy corresponding to the excitonic transition between *E1* and the thermally-populated light-hole level LH1.

The circles in Fig. 1(a) show the PL spectrum at 8.4 K in the presence of FIR radiation. The shape and the amplitude of this spectrum closely match the spectrum in Fig. 1(b). However, the energy of the *E1*-HH1 transition is unchanged from its unquenched 8.4 K value, indicating no change in the band gap. The absence of a significant blueshift indicates that the luminescence remains primarily excitonic. From these data, we deduce that the primary effect of the FIR irradiation is to heat luminescing excitons without heating the lattice.[15]

The solid lines in Figs. 2(a) and (b) show PL spectra in the absence of FIR radiation for the GRI 50 Å wide quantum well at 7.2 and 46 K, respectively. The three peaks in both spectra have been assigned[9] to excitonic PL from regions of the well with widths of 17, 16, and 15 ML [see inset of Fig. 2(b)]. At 7.2 K, the PL arises predominantly from excitons localized in regions that are 17 and 16 ML wide, with very little coming from the 15 ML regions. Most of the luminescing excitons are bound to intrinsic acceptors at this low temperature,[9] although there is a small contribution from free excitons as can be seen from the high energy shoulder of the central PL peak (16 ML) in Fig. 2(a). At 46 K, the integrated PL intensity is decreased and the 15 ML regions of the well are more significantly populated with luminescing excitons. The redshift due to band gap narrowing is much smaller for the GRI sample than the multiple-quantum-well sample (see Appendix A). Furthermore, above 30 K, the excitons become unbound from acceptors,[9] causing a 3 meV blueshift of the luminescence peak. The net result is that the PL peaks hardly shift as temperature increases from 7.2 to 46 K in the absence of FIR radiation.

The circles in Fig. 2(a) show the PL spectrum for the GRI sample at 7.2 K in the presence of FIR radiation. As for the multiple-quantum-well sample, the shape and the amplitude of this spectrum closely match the spectrum at a higher lattice temperature with no FIR irradiation [Fig. 2(b)]. The central peak of the FIR-quenched PL spectrum (circles) is at the same energy as the free-exciton shoulder on the central peak of the unquenched PL spectrum (solid line) in Fig. 2(a). This suggests that only the carriers are being heated and freed from acceptors, and that no lattice heating occurs to redshift the PL energy.

B. PL amplitudes vs carrier temperature

In the remainder of this paper, we will analyze carrier heating in the multiple-quantum-well sample. A comparison of the effects of higher lattice temperature and increasing FIR radiation intensity can be seen in Fig. 4. The open triangles show that the peak intensity of the heavy-hole excitonic PL (*E1*-HH1) decreases monotonically with increasing lattice temperature or FIR intensity. An exciton thermal dissociation model is used to fit the data in Fig. 4(a) (see Appendix A). The solid circles show that the peak intensity of the light-hole excitonic PL (*E1*-LH1) initially increases as the lattice temperature or FIR intensity is increased. This enhancement arises from the thermal excitation of heavy-hole excitons into the higher energy light-hole excitons.

At approximately 100 K, which corresponds approx-

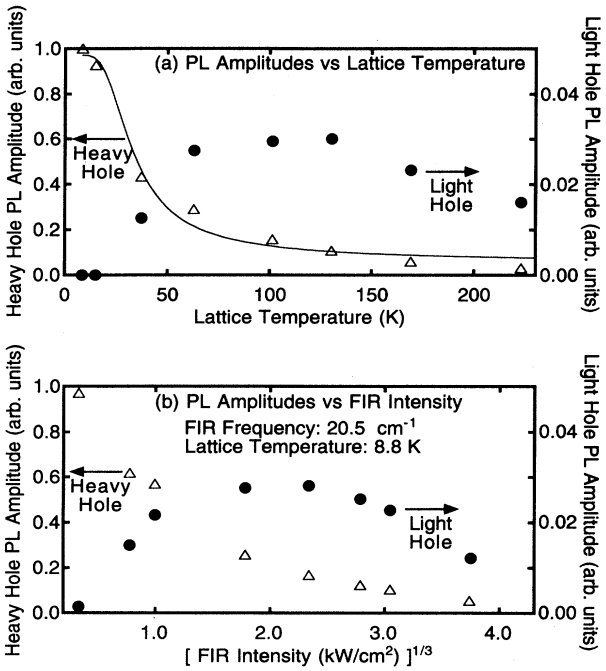

FIG. 4. Heavy-hole (triangles) and light-hole (disks) exciton PL amplitudes from the 100 Å wide $Al_{0.3}Ga_{0.7}As/GaAs$ multiple quantum wells versus (a) lattice temperature and (b) the cube root of the FIR intensity at a constant lattice temperature of 8.8 K. The fit in (a) arises from an exciton thermal dissociation model which is discussed in Appendix A. The FIR frequency is 20.5 cm^{-1}.

imately to the exciton ionization energy and the energy separating light and heavy holes [see Fig. 4(a)], the light-hole exciton PL intensity also begins to decrease as electron-hole correlations weaken and nonradiative traps strengthen at higher temperatures. The same effect can be seen in Fig. 4(b) above an FIR intensity of 16 kW/cm^2 and at a fixed lattice temperature of 8.8 K. In Fig. 4(b), the amplitude of the light-hole exciton PL drops faster with temperature than would be expected from the decrease in the heavy-hole exciton PL. This could be a result of a higher light-hole exciton temperature compared to the heavy-hole exciton temperature, but the uncertainty in the light-hole PL amplitudes does not allow any strong conclusions (see Appendix B).

In the absence of FIR radiation, the carrier temperature is assumed to be the same as the lattice temperature.[16] In the presence of FIR radiation [Fig. 4(b)], the carrier temperature is deduced by finding a lattice temperature [Fig. 4(a)] at which the heavy-hole PL amplitude is the same. The light-hole PL amplitude or the ratio of the light-hole to heavy-hole amplitudes also could be used and yields temperatures within approximately ±20% (see Appendix B). The success of such a comparison relies on the assumption that the PL amplitudes depend only on carrier temperature (see Appendix A).

The normalized PL amplitudes do not strongly depend on visible laser intensity. Various measurements were performed with the visible excitation intensity ranging from 2 to 34 W/cm^2 at the sample. Both the heavy- and light-hole PL amplitudes increased linearly with visible excitation intensity in this range. The PL peaks were slightly broadened at the higher excitation intensities. Normalizing the PL by the 9 K heavy-hole PL amplitude produced results that, for the most part, did not depend on the visible excitation intensity. The normalized heavy-hole PL amplitude, and hence the temperature extracted from it, did not depend on the visible excitation intensity. The normalized light-hole PL amplitudes were slightly larger for the higher visible excitation intensity runs (perhaps the light-hole PL amplitude is more sensitive to heating by the visible excitation—see Appendix B). Finally, the dependence of FIR-quenched PL on visible excitation intensity was measured at 14 cm^{-1}. The main effect of a higher visible excitation intensity (higher exciton density) was to enhance lattice heating for the higher FIR intensities. As a result, the heavy-hole PL, after the FIR pulse had ended, was also thermally quenched. In spite of the enhanced lattice heating at higher FIR and visible excitation intensities, the normalized PL amplitudes did not change significantly as the visible excitation intensity was increased from 2 to 34 W/cm^2.

C. Carrier heating vs FIR frequency

Figure 5 plots the carrier temperature versus FIR intensity for several fixed FIR frequencies between 15 and 110 cm^{-1} (2–13.7 meV). For a fixed FIR frequency, the carrier temperature increases roughly with the $\frac{1}{3}$ power of the FIR intensity, which is consistent with the measured temperature dependence of the energy relaxation time (see Sec. V B.). The power law fits yielded exponents slightly lower than expected, averaging 0.26 ± 0.03.

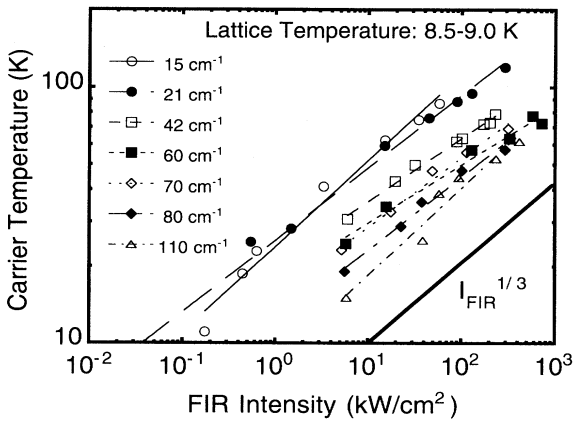

FIG. 5. Carrier temperature deduced from PL spectra of the 100 Å wide $Al_{0.3}Ga_{0.7}As/GaAs$ multiple quantum wells versus FIR intensity. The carrier temperature increases roughly as the 1/3 power of the FIR intensity at all frequencies. Heating is less efficient at the higher FIR frequencies.

This sublinear power dependence suggests that the carriers can relax faster at higher temperatures (i.e., higher FIR intensities). Furthermore, for a fixed FIR intensity, the carrier temperature decreases strongly with increasing FIR frequency. This frequency dependence is suggestive of Drude free-carrier absorption of FIR radiation.

IV. DRUDE ANALYSIS OF CARRIER HEATING

The FIR radiation heats photogenerated electrons and holes. We assume that the electrons and holes are at the same temperature. For the purposes of modeling, the electrons and holes can then be treated as an ensemble of particles with an absorption cross section $\overline{\sigma_{\rm abs}}$ equal to the average of the electron and hole absorption cross sections, and an energy relaxation rate $1/\overline{\tau_{\rm energy}}$ equal to the average of the electron and hole energy relaxation rates.

$$\overline{\sigma_{\rm abs}} = \frac{1}{2}\left(\sigma_{\rm abs}^{\rm electron} + \sigma_{\rm abs}^{\rm hole}\right) , \tag{4.1}$$

$$\frac{1}{\overline{\tau_{\rm energy}}} = \frac{1}{2}\left(\frac{1}{\tau_{\rm energy}^{\rm electron}} + \frac{1}{\tau_{\rm energy}^{\rm hole}}\right) . \tag{4.2}$$

We also assume that the electrons and holes share the same momentum relaxation time $\tau_{\rm mom}$.

The FIR pulses we use are much longer than the carriers' relaxation time, and thus may be treated as a steady-state excitation. Assuming that the power absorbed is equal to the power lost per carrier, the average energy relaxation time and absorption cross section are related by

$$P_{\rm abs} = I_{\rm FIR}\overline{\sigma_{\rm abs}} = P_{\rm lost} = \frac{k_B(T_C - T_L)}{\overline{\tau_{\rm energy}}} . \tag{4.3}$$

$I_{\rm FIR}$, $\overline{\sigma_{\rm abs}}$, k_B, T_C, T_L, and $\overline{\tau_{\rm energy}}$ are the FIR intensity, average absorption cross section, Boltzmann constant, carrier temperature, lattice temperature, and average energy relaxation time, respectively.

Grouping together all the measured quantities in Eq. (4.3) allows the product of the absorption cross section and energy relaxation time to be isolated. If we assume that the energy relaxation time depends only on carrier temperature, then the absorption cross section is proportional to $k_B(T_C - T_L)/I_{\rm FIR}$ when temperature is kept constant.

$$\overline{\sigma_{\rm abs}(\omega)}\ \ \overline{\tau_{\rm energy}(T_C)} = \frac{k_B(T_C - T_L)}{I_{\rm FIR}(\omega)} . \tag{4.4}$$

Within the Drude model, the absorption cross section for a free carrier is given by

$$\sigma_{\rm abs}(\omega) = \frac{4\pi e^2 \tau_{\rm mom}(T_C)}{cnm^*[1 + \tau_{\rm mom}(T_C)^2\omega^2]} , \tag{4.5}$$

where e, c, n, m^*, $\tau_{\rm mom}$, and ω are the electronic charge, speed of light, GaAs index of refraction, carrier effective mass, momentum relaxation time, and FIR angular frequency, respectively. The in-plane effective masses for the electron and heavy hole are $0.067m_0$ and $0.16m_0$,[17] respectively. The light hole has an even larger in-plane effective mass exceeding $0.18m_0$.[18] At the carrier temperatures reached in this experiment, the hole population was dominated by heavy holes. Therefore, we use the heavy-hole mass to determine the holes' contribution to the average absorption cross section.

We expect electrons to dominate FIR absorption due to their small masses, and hence large absorption cross sections. Though the electrons' small effective mass greatly enhances their contribution to the average absorption cross section, the average energy relaxation rate may in fact be dominated by hole relaxation rather than electron relaxation.[19]

Figure 6 plots $\overline{\sigma_{\rm abs}}\ \overline{\tau_{\rm energy}}$ [as given in Eq. (4.4)] as a function of FIR frequency. The fits using Eq. (4.5) are surprisingly good and allow energy and momentum relaxation times to be calculated for different carrier temperatures (see inset of Fig. 6). At the high frequencies used,

$$\lim_{\omega\tau_{\rm mom}>>1} \overline{\sigma_{\rm abs}(\omega)}\ \overline{\tau_{\rm energy}(T_C)} \propto \frac{\overline{\tau_{\rm energy}}}{\tau_{\rm mom}\ \omega^2} , \tag{4.6}$$

the data are close to the $1/\omega^2$ Drude absorption regime,[20] where it is difficult to extract $\overline{\tau_{\rm energy}}$ and $\tau_{\rm mom}$ separately. In fact, the lack of strong curvature in $\overline{\sigma_{\rm abs}}\ \overline{\tau_{\rm energy}}$ in Fig. 6 results in a relaxation time uncertainty of roughly a factor of four at 101 K and a factor of two at 36 K.[21] Therefore, the slight decrease in curvature at higher temperature (corresponding to an increase in $\tau_{\rm mom}$) is not conclusive. However, it is clear that $\overline{\sigma_{\rm abs}}\ \overline{\tau_{\rm energy}}$ decreases in

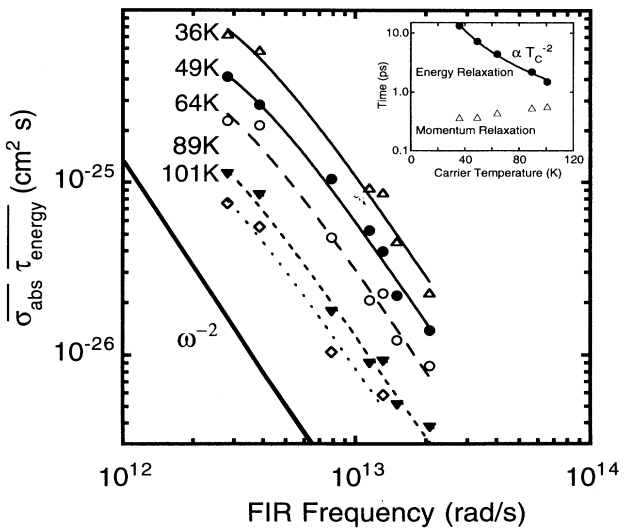

FIG. 6. Drude fit to the absorption cross section at different temperatures. Energy and momentum relaxation times extracted from the Drude fit are shown in the inset.

magnitude as temperature is increased. This result is a strong indication of the decrease of $\overline{\tau_{\text{energy}}}$ as temperature is increased. The decrease of the energy relaxation time with temperature confirms that carriers can relax faster at higher temperatures as more carriers have sufficient energy to emit fast-relaxation LO phonons.[22,23,6] The energy relaxation time exhibited a power law dependence on carrier temperature, with a fitted exponent of -1.97 ± 0.04 as can be seen in the inset of Fig. 6. Within this picture, the relaxation times extracted from the Drude fits include both electrons and holes.

V. DISCUSSION

A. Free-carrier FIR absorption in an excitonic system

The PL remains excitonic in nature for all the FIR frequencies and up to the highest FIR intensities. At the very highest intensities of 700 kW/cm^2, the FIR electric fields are 12 kV/cm, corresponding to a potential drop of 12 meV across an excitonic radius of 100 Å. Thus, the FIR electric fields are usually smaller than the static electric field binding the exciton together, and apparently are insufficient to field ionize the excitons. Similarly, heating excitons may diminish their population via thermal ionization, but will not defeat their dominance in PL from undoped samples even at room temperature.[7]

One might have expected that when the FIR photon energy matches the exciton binding energy (or the $1s$-$2p$ transition), nonthermal ionization (excitation), and hence resonant PL quenching would occur. The FIR photon energy was scanned[24] from 7 to 11 meV, but no resonant PL quenching was observed. This energy range encompasses most of the calculated and measured excitation energies for the heavy-hole exciton found in recent literature.[25] Photoluminescence excitation (PLE) measurements on our multiple-quantum-well sample[26] indicate a $1s$ to $2s$ energy splitting of approximately 10 meV, while PL measurements suggest this splitting is closer to 9 meV.

Though we expect very strong coupling of the FIR radiation to the $1s$-$2p$ transition in the 7–11 meV energy range, it is possible that the saturation of the $2p$ exciton state would not result in PL quenching of the $1s$ exciton. If both the radiative and nonradiative recombination of $2p$ excitons were weak, most of the $2p$ excitons would return to the $1s$ state to recombine radiatively and emit PL. Therefore, the quantum efficiency of the $1s$ excitonic PL would not be changed significantly, and the steady-state $1s$ excitonic PL would be unchanged even though the radiative lifetime could be increased dramatically by the resonant FIR pumping of the $2p$ state. Therefore, the $2p$ resonance could be best observed either by time-resolved PL, two-photon absorption,[27,28] or direct photoinduced FIR absorption.[29]

A second possible FIR resonance would involve the heavy- to light-hole transition induced by 11 meV FIR radiation (this transition is allowed due to strong valence band mixing).[30,31] This resonance was explored but not observed.

Given that the PL remains excitonic during the FIR pulses and that the carrier temperatures suggest that most of the carriers are still bound as excitons, it is surprising that the FIR-induced carrier heating could be accurately fitted by a simple Drude model. We believe that the resolution of this mystery lies in the fact that though excitons dominate PL, free carriers dominate FIR absorption. Excitonic luminescence is significantly stronger than band-to-band (free-carrier) radiative recombination, especially when the carrier temperature is below 100 K, where most of the carriers are still bound in excitons. On the other hand, the FIR coupling to excitons may be weak, which is supported by the lack of observed excitonic FIR resonances. Furthermore, if one assumes that the relatively high mobility of the free carriers allows them to dominate in absorbing FIR radiation, it is reasonable to suggest that the FIR radiation is heating the free carriers, which in turn heat the luminescing excitons. The steady-state picture involves a hot bath of free carriers, injected by the visible excitation radiation[32] and released by exciton dissociation, absorbing FIR radiation and heating the remaining excitons to their temperature. Excitonic PL is reduced as more excitons thermally ionize at higher temperatures and hot free electrons and free holes are less likely to bind as excitons. If the excitons are at the same temperature as the free-carrier bath, then the excitonic PL should reflect the free-carrier temperature and the Drude analysis should produce the correct relaxation times for the free carriers which are being heated by the FIR radiation. A quantitative analysis for this model has not been attempted.

B. Relaxation times

Numerous experiments have measured electronic relaxation rates in GaAs quantum heterostructures, and though most of the samples and experimental techniques are similar, the results vary significantly. Table I allows the results of this experiment to be compared with energy relaxation times measured by Refs. 6, 22, 19, 33 and 34.

Our experiment obtained energy relaxation times ranging from 11 ps at 40 K to 3 ps at 80 K. These times are shorter than those measured in other experiments, and the T_C^{-2} temperature dependence is much weaker. Except for Ref. 34, most experiments show a two order of magnitude decrease in energy relaxation time as temperature is raised from 40 to 80 K.

Though the temperature dependence of the energy relaxation time does not agree with other experiments, it does explain the power dependence of the carrier heating shown in Fig. 5. Equation (4.3) suggests that carrier temperature is related to the FIR intensity as follows:

$$T_C \propto I_{\text{FIR}} \overline{\tau_{\text{energy}}}. \tag{5.1}$$

Since $\overline{\tau_{\text{energy}}}$ is proportional to T_C^{-2}, Eq. (5.1) becomes

TABLE I. Energy relaxation times reported in various experiments using GaAs/$Al_{1-x}Ga_xAs$ quantum heterostructures. The relaxation times in this experiment include electron and hole relaxation, tend to be shorter and have weaker temperature dependence compared to the times measured in other experiments.

Source	Sample	Energy relaxation time τ_{energy}[a] (ps)		Carrier type	Sheet density (cm^{-2})
		$T_C = 40$ K	$T_C = 80$ K		
Ref. 19	260 Å MQW	2600	50	e	3×10^{11}
Ref. 19	260 Å MQW	180	2.7	h	7×10^{11}
Ref. 22	Two-dimensional electron gas (2-DEG)	4000		e	$(2-8) \times 10^{11}$
Ref. 33	2-DEG	100	1	e	3.9×10^{11}
Ref. 34	150 Å MQW	100	10	e	2.5×10^{11}
Ref. 6	2-DEG		10–30	e	3.3×10^{11}
Černe *et al.*	100 Å MQW	11[b]	3[b]	e, h	3×10^{9}

[a]These experiments report energy relaxation rates P_{lost}, electron-LO phonon scattering times τ_{LO}, or total energy relaxation times τ_{energy}. For temperatures where energy relaxation via LO phonons dominates, these three quantities are related by $P_{lost} = (E_{LO}/\tau_{LO})e^{-E_{LO}/k_BT_C} = \{[k_B(T_C - T_L)]/\tau_{energy}\}$ where E_{LO} is the LO phonon energy.
[b]This energy relaxation time is averaged over the electrons and holes. See Eq. (4.2).

$$T_C \propto I_{FIR} T_C^{-2} \quad \rightarrow \quad T_C^3 \propto I_{FIR}. \tag{5.2}$$

This result is consistent with Fig. 5, which shows that the carrier temperature grows as the 1/3 power of FIR intensity.

Though the uncertainty in the energy relaxation times is large (up to a factor of four at 100 K), and the values at higher temperatures are within the range measured by other experiments, there are several key differences that distinguish this experiment from the rest, which may help explain the discrepancies. The density of photoexcited carriers in our experiment is only 3×10^9 cm^{-2}, much smaller than in the doped samples studied by others. A lower carrier density tends to reduce hot optical phonon reabsorption by carriers,[35] and should result in faster energy relaxation rates for the carriers. Furthermore, since the FIR radiation is heating holes as well as electrons, the overall relaxation times may be shortened by the faster relaxation of holes.[19] In calculating the FIR absorption cross section for holes, we neglected the light holes and valence band mixing. Including such contributions would tend to increase the average effective mass for the holes, and hence would tend to reduce their average absorption cross section. As a result of neglecting the valence band complexities, we have probably overestimated the average absorption cross section, which would result in smaller energy relaxation times.

Whereas the energy relaxation time strongly decreases with increasing temperature, the momentum relaxation time increases slightly in that same temperature range (see inset Fig. 6). Though several mechanisms could explain the increase in τ_{mom} with temperature (corresponding to a decrease in interface roughness scattering[36] or a decrease in electron-hole scattering[37] as carrier temperature is increased) this trend is too weak to be substantiated by the data. The momentum relaxation times of approximately 0.5 ps suggest a very low electron mobility of 13 000 V/cm s, which could be a result of strong excitonic electron-hole correlations leading to strong scattering.

VI. CONCLUSION

Excitonic PL from $Al_xGa_{1-x}As$ quantum wells at low temperature clearly indicates that free-carrier heating is the dominant effect of FIR radiation. At maximum intensities of 700 kW/cm^2 or 12 kV/cm, the FIR radiation raises the carrier temperature in the multiple-quantum-well sample to over 100 K, and lowers the inelastic relaxation time to 1 ps. The average free-carrier energy relaxation time is inversely proportional to the carrier temperature squared. Though excitons dominate the luminescence, free carriers play a much stronger role in FIR absorption.

The fact that no exciton resonances were observed using steady-state PL may be more indicative of the experimental limitations rather than the weakness of FIR coupling to excitons. We hope to use other measurement techniques to observe FIR-excited excitons.

The dominance of FIR-induced carrier heating could be minimized if the carriers' degrees of freedom were further reduced by applying a magnetic field or increasing localization in lower dimensional structures such as quantum wires and dots. A further advantage of investigating lower dimensional quantum structures would be the possibility of examining the phonon bottleneck. We hope to distinguish additional effects of FIR radiation on carriers in quantum wells, e.g., ac Stark shift, resonant exciton ionization, and intersubband transitions, in future experiments.

Despite the qualitative nature of this experiment, the Drude model could be applied to the FIR intensity and frequency dependence of the carrier heating to obtain energy and momentum relaxation times. This experiment not only resolves the dominance of carrier heating in quenching PL in quantum wells by intense FIR radiation, but also underscores the need to include this effect when probing the many other exciting properties of these structures.

ACKNOWLEDGMENTS

The authors gratefully acknowledge the discussions with J.N. Heyman, N.G. Asmar, K. Unterrainer, J. Worlock, A. Pinczuk, and K.A. Collins. We would also like to thank D.P. Enyeart and J.R. Allen at the Center for Free-Electron Laser Studies for their technical support. This work has been supported by the NSF Science and Technology Center for Quantized Electronic Structures DMR 91-20007, ONR N00014-K-0692, AFOSR 88-0099, DFG-SFB6, and the Alfred P. Sloan Foundation (MSS).

APPENDIX A: TEMPERATURE DEPENDENCE OF PL

As the temperature of the samples is increased, the PL energy and intensity decrease. The decrease in energy is due to the band gap narrowing at higher lattice temperatures. In a bulk material, the temperature dependence of the energy gap $E_g(T)$ is[38]

$$E_g(T) = E_g(0) - \frac{\alpha T^2}{T+\beta} , \tag{A1}$$

where $\alpha = 5.4 \times 10^{-4}$ eV/K and $\beta = 204$ K for GaAs. This will clearly affect photoluminescence in quantum wells as can be seen in Fig. 1. The multiple-quantum-well sample follows this behavior closely as the PL energy shifts 114 meV from 8 to 300 K. The GRI sample, however, exhibits a much smaller shift of only 14 meV over the same temperature range.

The temperature dependence of the PL intensity is more complicated. At low temperatures (< 20 K) the increase in PL is dominated by localization of excitons in interface defects and impurities. This localization in the quantum-well plane allows partial violation of momentum conservation in radiative recombination, and therefore increases the overall luminescence intensity.[7,8,39] Similarly, the distribution of free excitons at a higher temperature results in an enhanced occupation of higher center of mass momentum states away from $k_{\text{exciton}} = 0$. These more energetic excitons cannot radiatively recombine without violating momentum conservation, and therefore the radiative recombination rate[12] and the PL efficiency decrease. At high temperatures ($\approx$100–300 K) PL decreases exponentially with temperature as nonradiative recombination mechanisms become thermally activated.[11]

In the intermediate temperature range where most of our measurements were made, the change in PL intensity mainly can be attributed to thermal dissociation of excitons.[11] The temperature dependence of the PL intensity can therefore be modeled by[11]

$$I_{\text{PL}}(T_C) = \frac{A}{1 + Be^{-E_X/k_B T_C}} , \tag{A2}$$

where E_X is the exciton binding energy. This calculated dependence is fitted to the heavy-hole PL in Fig. 4(a). Not only does this fit neglect the low and high temperature behavior mentioned earlier, it also ignores thermal pumping of the light-hole population from the heavy-hole state. In spite of these shortcomings, this simple model fits reasonably well for intermediate temperatures and produces a fitted heavy-hole exciton binding energy of 9.0 ± 1.5 meV, which agrees reasonably well with the values calculated by Refs. 40–42.

APPENDIX B: EXPERIMENTAL MEASUREMENT OF TEMPERATURE USING PL

In this experiment there are several types of PL measurement from which carrier temperature could be obtained. Carrier temperature could be deduced from the normalized heavy-hole PL amplitude, the normalized light-hole PL amplitude, the ratio of light- and heavy-hole PL, or the slope of the Boltzmann-like tail on the higher energy side of the PL peaks. The accuracy and agreement of these methods will be discussed in this appendix.

Since the heavy-hole exciton PL amplitude is closely related to carrier temperature (Appendix A), we have been able to use this feature to estimate carrier temperature in our experiment. Since all the PL spectra were normalized by the 9 K heavy-hole exciton PL amplitude, measurements that were taken at different times and under slightly different conditions could be compared directly. The heavy-hole PL amplitude provided a consistent measurement that was reproducible to within 10% from day to day (i.e., the normalized heavy-hole amplitude was the same for a given lattice temperature even though the excitation intensity, collection efficiency, sample alignment, and other experimental parameters may have changed).

The light-hole exciton PL amplitude also provided a measure of the carrier temperature. Compared to the heavy-hole PL, the light-hole PL peaks are much smaller and more limited by noise. Unlike the normalized heavy-hole PL, the normalized light-hole PL is more sensitive to excitation intensity. This problem is aggravated by the fact that the light-hole PL measurement is separated from the normalizing heavy-hole PL amplitude by several minutes, which allowed small drifts in excitation intensity to affect the results. Higher temperatures are more difficult to measure since the light-hole PL amplitudes are nearly constant at approximately 100 K. Despite these difficulties, the temperature measured using the normalized light-hole PL amplitude is within $\pm 20\%$ of the value measured with the heavy-hole PL for FIR frequencies above 40 cm^{-1}. At the lowest two FIR frequencies (15 and 20.5 cm^{-1}), the discrepancy between the light- and heavy-hole PL temperature estimates could be as high as 50%. This discrepancy is clearly seen in Fig. 4(b), where the light-hole PL amplitudes suggest significantly higher carrier temperatures than the heavy-hole PL amplitudes.

Despite the difficulties in using the light-hole PL amplitude to measure the carrier temperature, the ratio of the light-hole PL to the heavy-hole PL provided a reasonably

good estimate of carrier temperature. The temperatures obtained by this PL ratio agreed with the measurements using the heavy-hole PL amplitude to within 20%.

Similar results were obtained by comparing the high energy PL tails, which are approximately Boltzmann-like and reproduced the actual temperature to within a constant factor. Though the exciton distribution may have been Boltzmann-like, momentum conservation reduces the radiative recombination of delocalized higher energy excitons and thus modifies the high energy PL tail. Due to decreased PL from higher energy excitons, the temperature measured from the high energy PL tail was consistently reduced by a factor of 1/4 compared to the lattice temperature. Though all four methods lead to approximately the same results shown in Fig. 5, the heavy-hole PL amplitude is the dominant indicator since it proved to be the simplest and most robust measurement of exciton temperature.

[1] J.N. Heyman, K. Craig, B. Galdrikian, M.S. Sherwin, K. Campman, P.F. Hopkins, S. Fafard, and A.C. Gossard, Phys. Rev. Lett. **72**, 2183 (1994).

[2] A. Markelz, N.G. Asmar, E.G. Gwinn, M.S. Sherwin, C. Nguyen, and H. Kroemer, Semicond. Sci. Technol. **9**, 634 (1994).

[3] K. Craig, C.L. Felix, J.N. Heyman, A.G. Markelz, M.S. Sherwin, K.L. Campman, P.F. Hopkins, and A.C. Gossard, Semicond. Sci. Technol. **9**, 627 (1994).

[4] B. Birnir, B. Galdrikian, R. Cramer, and M.S. Sherwin, Phys. Rev. B **47**, 6795 (1993).

[5] M.S. Sherwin, in *Quantum Chaos*, edited by G. Casati and B.V. Chirikov (Cambridge University Press, Cambridge, 1994).

[6] N.G. Asmar, A.G. Markelz, E.G. Gwinn, P.F. Hopkins, and A.C. Gossard, Semicond. Sci. Technol. **9**, 828 (1994).

[7] J. Christen and D. Bimberg, Phys. Rev. B **42**, 7213 (1990).

[8] R.F. Schnabel, R. Zimmerman, D. Bimberg, H. Nickel, R. Lösch, and W. Schlapp, Phys. Rev. B **46**, 9873 (1992).

[9] D. Bimberg, F. Heinrichsdorff, and R.K. Bauer, J. Vac. Sci. Technol. B **10**, 1793 (1992).

[10] S.M. Quinlan, A. Nikroo, M.S. Sherwin, M. Sundaram, and A.C. Gossard, Phys. Rev. B **45**, 9428 (1992).

[11] De-Sheng Jiang, H. Jung, and K. Ploog, in *Proceedings of the Workshop on Physics of Superlattices and Quantum Wells,* edited by C.-H. Tsai, X. Wang, X.-C. Shen, and X.-L. Lei (Singapore, World Scientific, 1989), pp. 217–231.

[12] J. Feldmann, G. Peter, E.O. Göbel, P. Dawson, K. Moore, C. Foxon, and R.J. Elliott, Phys. Rev. Lett. **59**, 2337 (1987).

[13] R. Köhrbrück, S. Munnix, D. Bimberg, D.E. Mars, and J.N. Miller, J. Vac. Sci. Technol. B **8**, 798 (1990).

[14] Etalon effects cause the FIR intensity in the sample to vary drastically with FIR frequency. In this case, however, the optic fiber is less than 200 μm away from the face of the sample, which probably disrupts reflections at that surface and eliminates etalon effects.

[15] At the highest FIR intensity, the lattice temperature remains below 15 K. Note that there are subtle differences between the 8.4 K FIR-irradiated spectrum and the 96 K spectrum. In particular, the PL linewidth is broader at 96 K, perhaps due to increased phonon scattering.

[16] This assumption is reasonable for the 36–100 K temperature range used in our calculations, but begins to fail at lower temperatures (Ref. 8) where the carriers tend to have a higher temperature than the lattice.

[17] M. Nithisoontorn, R. Dum, K. Unterrainer, J.S. Michaelis, E. Gornik, N. Sawaki, and H. Kano, Surf. Sci. **267**, 505 (1992).

[18] M. Nithisoontorn, K. Unterrainer, S. Michaelis, E. Gornik, N. Sawaki, and H. Kano, *Quantum-Well and Superlattice Physics III, San Diego, CA, 1990* (Proceedings of the SPIE- The International Society for Optical Engineering, 1990), Vol. 1283, p. 310.

[19] J. Shah, A. Pinczuk, A.C. Gossard, and W. Wiegmann, Phys. Rev. Lett. **54**, 2045 (1985).

[20] S. Perkowitz, J. Phys. Chem. Solids **32**, 2267 (1971).

[21] The uncertainties obtained from the fits in Fig. 6 were roughly $\pm 20\%$ and $\pm 15\%$ for $\overline{\tau_{\text{energy}}}$ and τ_{mom}, respectively, which significantly underestimate the overall uncertainty.

[22] K. Hirakawa and H. Sakaki, Appl. Phys. Lett. **49**, 889 (1986).

[23] K. Hirakawa, M. Grayson, D.C. Tsui, and Ç. Kurdak, Phys. Rev. B **47**, 16 651 (1993).

[24] The FIR energy was scanned in increments of 0.01 meV at a constant intensity of approximately 1 kW/cm^2. The relative power at the sample was calibrated using the Thomas Keating detector mentioned in Sec. II B. The entire FIR beam path was enclosed by a dry, nitrogen-purged environment to eliminate FIR absorption by water vapor.

[25] References 40 and 41 determined the heavy-hole exciton binding energy to be approximately 9 meV, while Refs. 43 and 44 report higher binding energies of 14 and 20 meV, respectively. More recent experiments using (PLE) (Refs. 45 and 46) suggest that the heavy-hole exciton binding energy may be closer to 10 meV. Reference 42 provides an empirical formula from which we obtain a heavy-hole exciton binding energy of 9.6 ± 0.3 meV for our sample. Reference 47 calculates the $1s$-$2s$ and $1s$-$2p$ energy splittings to be 6.9 and 6.6 meV, respectively, which does not agree with the $1s$-$2s$ splitting that we measured and is below the energy range used in our FIR scans.

[26] The PLE measurements on the multiple-quantum-well sample were made by S. Fafard at UCSB.

[27] K. Tai, A. Mysyrowicz, R.J. Fischer, R.E. Slusher, and A.Y. Cho, Phys. Rev. Lett. **62**, 1784 (1989).

[28] M. Nithisoontorn, K. Unterrainer, S. Michaelis, N. Sawaki, E. Gornik, and H. Kano, Phys. Rev. Lett. **62**, 3078 (1989).

[29] M. Olszakier, E. Ehrenfreund, E. Cohen, J. Bajaj, and G.J. Sullivan, Phys. Rev. Lett. **62**, 2997 (1989).

[30] Y.C. Chang and R.B. James, Phys. Rev. B **39**, 12 672 (1989).

[31] P.C.M. Planken, M.C. Nuss, I. Brener, K.W. Goosen, M.S.C. Luo, S.L. Chuang, and L. Pfeiffer, Phys. Rev. Lett. **69**, 3800 (1992).

[32] Unfortunately, no resonant excitation could be performed to create only cold excitons directly. However, we think that the rapid relaxation of hot free carriers into the lowest energy exciton states in the quantum well should allow our results to approach those obtained under resonant exciton

creation.
[33] K. Tsubaki, A. Sugimura, and K. Kumabe, Appl. Phys. Lett. **46**, 764 (1985).
[34] C.H. Yang, J.M. Carlson-Swindle, S.A. Lyon, and J.M. Worlock, Phys. Rev. Lett. **55**, 2359 (1985).
[35] P. Brockmann, J.F. Young, P. Hawrylak, and H.M. van Driel, Phys. Rev. B **48**, 11 423 (1993).
[36] H. Sakaki, T. Noda, K. Hirakawa, M. Tanaka, and T. Matsusue, Appl. Phys. Lett. **51**, 1934 (1987).
[37] H. Akiyama, T. Matsusue, and H. Sakaki, Phys. Rev. B **49**, 14 523 (1994).
[38] Thurmond, J. Electrochem. Soc. **122**, 1133 (1975).
[39] M.A. Herman, D. Bimberg, and J. Christen, J. Appl. Phys. **70**, R1 (1991).
[40] R.C. Miller, D.A. Kleinman, W.T. Tsang, and A.C. Gossard, Phys. Rev. B **24**, 1134 (1981).
[41] R.L. Greene and K.K. Bajaj, Solid State Commun. **45**, 825 (1983).
[42] G. Oelgart, M. Proctor, D. Martin, F. Morier-Genaud, F.-K. Reinhart, B. Orschel, L.C. Andreani, and H. Rhan, Phys. Rev. B **49**, 10 456 (1994).
[43] B.A. Vojak, N. Holonyak, Jr., W.D. Laidig, K. Hess, J.J. Coleman, and P.D. Dapkus, Solid State Commun. **35**, 477 (1980).
[44] J.C. Maan, G. Belle, A. Fasolino, M. Altarelli, and K. Ploog, Phys. Rev. B **30**, 2253 (1984).
[45] D.W. Kim, Y.A. Leem, S.D. Yoo, D.H. Woo, D.H. Lee, and J.C. Woo, Phys. Rev. B **47**, 2042 (1993).
[46] M. Gurioli, J. Martinez-Pastor, M. Colocci, A. Bossacchi, S. Franchi, and L.C. Andreani, Phys. Rev. B **47**, 15 755 (1993).
[47] R.L. Greene, K.K. Bajaj, and D.E. Phelps, Phys. Rev. B **29**, 1807 (1984).